Superfluid Spin Transport Through Easy-Plane Ferromagnetic Insulators

So Takei and Yaroslav Tserkovnyak
Department of Physics and Astronomy, University of California, Los Angeles, California 90095, USA
(Received 1 November 2013; published 2 June 2014)

Superfluid spin transport—dissipationless transport of spin—is theoretically studied in a ferromagnetic insulator with easy-plane anisotropy. We consider an open geometry where the spin current is injected into the ferromagnet from one side by a metallic reservoir with a nonequilibrium spin accumulation and ejected into another metallic reservoir located downstream. Spin transport is studied using a combination of magnetoelectric circuit theory, Landau-Lifshitz-Gilbert phenomenology, and microscopic linear-response theory. We discuss how spin superfluidity can be probed in a magnetically mediated negative electron-drag experiment.

DOI: 10.1103/PhysRevLett.112.227201 PACS numbers: 75.76.+j, 75.70.Ak, 75.78.-n, 85.75.-d

Introduction.—An important goal in the field of spintronics is to understand how spin, a quantum-mechanical unit of magnetism, can be exploited for information transport, data storage, and processing. While conventional spintronics [1] relying solely on conduction electrons in metals and semiconductors as carriers of spins still faces difficulties associated with fast spin relaxation and significant Joule heating, a promising alternative that combines conventional spintronics with coherent spin-wave dynamics in magnetic insulators has recently emerged [2]. Magnetic insulators can also transport spin information via magnons [3], the quantum of spin waves that also carries a unit of angular momentum. This emerging field of magnon spintronics may alleviate the obstacles present within the conventional schemes. The possibility to investigate spin transport in magnetic insulators also opens a new venue for their experimental probes.

Integrating magnetic insulators into spintronic devices raises interesting possibilities that stem from the bosonic nature of the spin-carrying magnons. These magnons can form a Bose-Einstein condensate, which has been observed in some magnetic insulators including $TlCuCl_3$ [4], Cs_2CuCl_4 [5], and $Y_3Fe_5O_{12}$ (YIG) films [6]. A closely related phenomenon is superfluidity, which is another general property of bosonic quantum matter at low temperatures. In magnetic systems, this raises the possibility of spin superfluidity, i.e., a dissipationless macroscopic transport of spin [7]. In the past, the concept was used to explain unusually fast spin relaxation in ^{3}He-A [8] and invoked to interpret the coherence of a nonuniformly precessing state of ^{3}He-B [9]. Spin superfluidity has also been studied in Bose-condensed excitonic fluids [10]. While the absence of strict conservation laws for spin rules out faithful analogy to conventional mass superfluidity [11], it was demonstrated that the analogy can still be useful if the violation of conservation law is weak [10]. The generation of dissipationless spin current has received attention in the past in metallic systems with noncollinear magnetic order [12], *p*-doped semiconductors [13], and two-dimensional electron systems with Rashba spin-orbit coupling [14].

In this Letter, we theoretically investigate how superfluid spin transport can be realized and detected in magnetic-insulator-based hybrid structures. The notion of superfluid spin transport here is closely related to Ref. [12]. In this Letter, we focus on the pertinent spin-transfer physics at the ferromagnet|metal interfaces (including thermally activated spin currents), which is related to well-established and independently measurable quantities such as the spin-mixing conductance and the spin Hall angle. We identify the importance of global magnetic precession and the associated relaxation of spin superfluid by Gilbert damping. Specifically, we consider a ferromagnetic insulator with easy-plane anisotropy attached on the two sides by metallic reservoirs that act as the source and the drain for spin current (see Fig. 1). In an open geometry, superfluid spin transport is achieved by maintaining a spiral magnetic texture in the ferromagnet, along with a self-consistent magnetic precession within the easy plane through a steady injection of angular momentum at the source and its depletion by spin

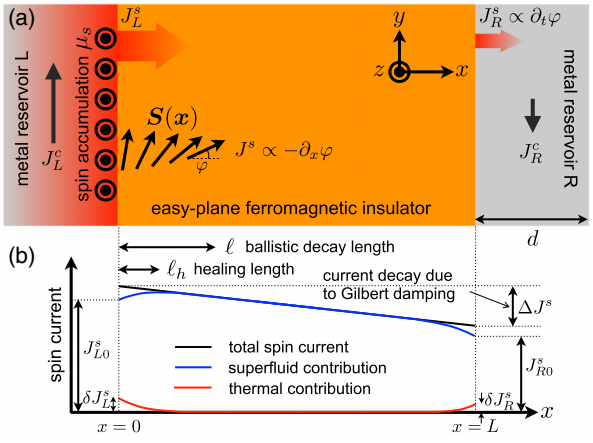

FIG. 1 (color online). (a) Schematic of the hybrid structure for realizing spin superfluidity. (b) A schematic plot showing the spatial distribution of the condensate and thermal contributions to the spin currents in the presence of Gilbert damping. See text for a detailed discussion.

 © 2014 American Physical Society

pumping [15] at the drain. The spin injection at the source and its ejection at the drain have two contributions: coherent spin-transfer torque [16] and thermally activated spin current mediated by magnons. We establish the length scales involved in the conversion of the thermal contribution into a superflow, with its eventual relaxation due to Gilbert damping. The resultant spin current can be probed in a magnetically mediated negative electron-drag experiment, similar to the proposal in Ref. [17], facilitated by the spin Hall effect at the ferromagnet|normal-metal contacts.

Superfluid spin transport.—Before pursuing a more rigorous microscopic calculation, we first outline the essential semiclassical aspects of superfluid spin transport (see Fig. 1). We start at zero temperature, where spin current in the ferromagnet cannot be transported by magnons. A ferromagnet of length L (occupying $0 < x < L$) is sandwiched between two metallic reservoirs occupying $-\infty < x < 0$ and $L < x < \infty$. We assume full translational symmetry along the interface (yz) plane, axial symmetry about the z axis, and take the easy plane in the xy plane. The energy for the ferromagnet can be written as $H_F = \int d^3\boldsymbol{x}[A(\nabla \boldsymbol{n}(\boldsymbol{x}))^2 + K n_z(\boldsymbol{x})^2]/2$, where A and K parametrize the exchange stiffness and anisotropy, respectively, and $\boldsymbol{n}(\boldsymbol{x})$ is the unit vector along the local spin density $\boldsymbol{s}(\boldsymbol{x})$. We parametrize $\boldsymbol{n}$ by the azimuthal angle φ and its z projection $\boldsymbol{n} = (\sqrt{1-n_z^2}\cos\varphi, \sqrt{1-n_z^2}\sin\varphi, n_z)$ and describe its classical dynamics using the Landau-Lifshitz-Gilbert (LLG) equation $(1 + \alpha \boldsymbol{n}\times)\dot{\boldsymbol{n}} = -\boldsymbol{n} \times \partial_s H_F$, where α is a dimensionless damping constant that accounts for magnetic losses in the ferromagnet bulk. In the strong-anisotropy and long-wavelength limit (i.e., $\lambda \gg \sqrt{A/K}$), the LLG equation can be expanded to lowest order in n_z and gradients of φ:

$$\dot{\varphi} = K n_z/s + \alpha \dot{n}_z, \qquad \dot{n}_z = A\nabla^2\varphi/s - \alpha\dot{\varphi}, \tag{1}$$

where $s \equiv |\boldsymbol{s}(\boldsymbol{x})|$ is assumed to be fixed at its saturation value. For $\alpha = 0$, Eqs. (1) are a magnetic analog of the Josephson relations for superfluidity. The first term on the right-hand side of the second equation defines the supercurrent density (for the z projection of spin) as $\boldsymbol{J}^s(\boldsymbol{x}) = -A\nabla\varphi(\boldsymbol{x})$, and the spin waves can be shown to have a soundlike linear spectrum as in a superfluid with the speed $v = \sqrt{AK}/s$. From Eqs. (1), we identify φ and sn_z as canonically conjugate variables, with the long-wavelength Hamiltonian given by $H_F \approx \int d^3\boldsymbol{x}[A(\nabla\varphi)^2 + K n_z^2]/2$.

Perturbing a monodomain ferromagnet by a nonequilibrium z-axis spin accumulation in the left reservoir, the magnet's spins cant out of the plane and acquire a nonzero n_z, which, in turn, triggers a precession of the magnetic order about the z axis by virtue of Eqs. (1). A steady-state solution for n_z and φ can be written as $n_z(\boldsymbol{x}, t) \equiv \text{const} = n_z$ and $\varphi(\boldsymbol{x}, t) = \varphi(x) + \Omega t$, where $\Omega = K n_z/s$ is the precession frequency and $\varphi'' = (\alpha s/A)\Omega$. According to the translational symmetry along the interfaces, we are considering solutions that are independent of (y, z). The magnetization canting n_z and the condensate spin-current density flowing through the ferromagnet in the x direction J^s must be found according to the appropriate boundary conditions at $x = 0, L$. To that end, we employ the magnetoelectric circuit theory [15], as follows.

The spin-current density injected into the ferromagnet from the left reservoir is given by $\boldsymbol{J}_L^s = (\Im g_L^{\uparrow\downarrow} + \Re g_L^{\uparrow\downarrow}\boldsymbol{n}\times)(\tilde{\boldsymbol{\mu}}_s \times \boldsymbol{n})/4\pi$, where $\Re g_r^{\uparrow\downarrow}$ and $\Im g_r^{\uparrow\downarrow}$ are, respectively, the real and imaginary parts of the spin-mixing conductance $g_r^{\uparrow\downarrow} \equiv \Re g_r^{\uparrow\downarrow} + i\Im g_r^{\uparrow\downarrow}$ associated with the ferromagnet|reservoir-r interface. $\tilde{\boldsymbol{\mu}}_s$ has two contributions: $\tilde{\boldsymbol{\mu}}_s \equiv \boldsymbol{\mu}_s - \hbar \boldsymbol{n} \times \dot{\boldsymbol{n}}$ corresponding to spin-transfer torque and spin pumping, respectively. Here, $\boldsymbol{\mu}_s = \mu_s \boldsymbol{e}_z$ is the nonequilibrium spin accumulation in the left reservoir. We, thus, have in our linearized theory: $\boldsymbol{n} \times \dot{\boldsymbol{n}} \approx \Omega \boldsymbol{e}_z$ and $J_L^s = g_L^{\uparrow\downarrow}(\mu_s - \hbar\Omega)/4\pi$ for the z component of the spin current. A similar analysis at the right interface gives the spin current injected into the right reservoir: $J_R^s = g_R^{\uparrow\downarrow}\hbar\Omega/4\pi$. With finite damping, the amount of spin supercurrent dissipated in the ferromagnet of length L is given by $\Delta J^s \equiv J_L^s - J_R^s = \alpha s \Omega L$. Imposing the continuity of spin current at the boundaries according to the circuit theory, we then obtain

$$\Omega = \frac{\mu_s}{\hbar}\frac{g_L^{\uparrow\downarrow}}{g_L^{\uparrow\downarrow} + g_R^{\uparrow\downarrow} + g_\alpha}, \quad J_R^s = \frac{\mu_s}{4\pi}\frac{g_L^{\uparrow\downarrow} g_R^{\uparrow\downarrow}}{g_L^{\uparrow\downarrow} + g_R^{\uparrow\downarrow} + g_\alpha}, \tag{2}$$

where $g_\alpha \equiv 4\pi\alpha s L/\hbar$. This is a central result of this work. Note that the supercurrent decays algebraically as a function of the ferromagnet's length L in the presence of Gilbert damping. For spin transport mediated solely by magnons [17], the spin current is expected to decay exponentially over the magnon diffusion length $\lambda_{\text{sd}} \sim v\sqrt{\tau\tau^*}$, τ (τ^*) being the decay (scattering) mean free times. The detection of appreciable spin current for $L \gg \lambda_{\text{sd}}$ should be evidence of spin superfluidity.

Microscopic theory.—In order to account for finite-temperature corrections to the above results, we proceed to develop a linear-response theory for a concrete microscopic model. To that end, consider a ferromagnet with spins arranged on a cubic lattice. With the xy easy plane, its energy is $\hat{H}_F = -(J/2)\sum_{\langle \boldsymbol{ij}\rangle} \boldsymbol{S_i} \cdot \boldsymbol{S_j} + (D/2)\sum_{\boldsymbol{i}} S_{z\boldsymbol{i}}^2$, where $J > 0$ is the exchange integral, $D > 0$ is the anisotropy energy, and $\boldsymbol{S_i}$ is the local spin in units of $\hbar$. Sites are labeled by $\boldsymbol{i}, \boldsymbol{j}$ and nearest-neighbor sites are denoted by $\langle \boldsymbol{ij}\rangle$. The low-energy behavior of the system is described by replacing the spin $\boldsymbol{S_i}$ on lattice site $\boldsymbol{i}$ with a continuum spin density, $\boldsymbol{S}(\boldsymbol{x}) \approx \boldsymbol{S_i}/a^3$, that varies slowly in space. Owing to the axial symmetry about the z axis, it is useful to parametrize the spin density using two slowly varying fields, its azimuthal angle $\varphi(\boldsymbol{x})$ and z component $S_z(\boldsymbol{x})$. Retaining terms up to quadratic order in small quantities, the long-wavelength (quantum) Hamiltonian in the case of a strong easy-plane anisotropy becomes

$$\hat{H}_F \approx \int d^3\boldsymbol{x}[A(\nabla\hat{\varphi})^2 + K\hat{n}_z^2]/2, \tag{3}$$

where $A = JS^2/a$, $K = DS^2/a^3$, and $\hat{n}_z(\boldsymbol{x}) = a^3\hat{S}_z(\boldsymbol{x})/S$. The fields $\hat{\varphi}(\boldsymbol{x})$ and $\hat{S}_z(\boldsymbol{x})$ are canonically conjugate variables obeying $[\hat{\varphi}(\boldsymbol{x}), \hat{S}_z(\boldsymbol{y})] = i\delta(\boldsymbol{x}-\boldsymbol{y})$. We have dropped terms in Eq. (3) that are higher order in $J(a/\lambda_T)^2/D \ll 1$, where λ_T is the thermal magnon wavelength at temperature T. Using the long-wavelength magnon velocity $v = \sqrt{JD}aS/\hbar$ and the thermal wavelength $\lambda_T \sim \hbar v/k_B T$, the above inequality gives a condition on the relevant temperature regime: $T \ll DS/k_B \equiv T_D$. We generalize our results to the opposite, high-temperature regime $T_D \ll T$ (where magnons become circular) at a later point.

The metallic reservoirs on the left ($r = L$) and right ($r = R$) are modeled as free electron gases with dispersion $\epsilon_{\boldsymbol{k}k_x r} = \hbar^2(|\boldsymbol{k}|^2 + k_x^2)/2m_r$, where m_r denotes the effective electron masses for the two reservoirs, and $\boldsymbol{k}$ (k_x) labels the wave number parallel (normal) to the interface plane. The nonequilibrium spin accumulation is induced in the left reservoir, where the chemical potentials of the two spin species are separated by μ_s. The spin-dependent distribution function for the left reservoir is, thus, given by $n_{\rm FD}(\varepsilon - \sigma\mu_s/2)$, where $n_{\rm FD}(x) = [e^{\beta(x-\mu)} + 1]^{-1}$, with $\beta = (k_B T)^{-1}$ and chemical potential μ, and $\sigma = +(-)$ corresponds to the up-spin (down-spin) electrons. Both spin species in the right reservoir obey $n_{\rm FD}(\varepsilon)$. We take the spin quantization axis for the spin accumulation along the z axis. (For the case of in-plane spin accumulation, see the Supplemental Material [18].)

We suppose that the ferromagnet magnetization and electron spin density at each interface couple via an sd-type exchange interaction. For strong anisotropy, the interaction Hamiltonian up to $\mathcal{O}(\hat{S}_z/S)$ can be written as $\hat{V} = \sum_r \hat{V}_r$, with

$$\hat{V}_r = \eta_r \int d^2\boldsymbol{r}\left[\frac{\tilde{S}e^{-i\hat{\varphi}(x_r)}}{2}\hat{s}_r^+(x_r) + \text{H.c.} + \hat{S}_z(x_r)\hat{s}_r^z(x_r)\right], \tag{4}$$

where η_r is the exchange coupling, $\tilde{S} = S/a^3$, and $x_{L,R} = 0, L$. The reservoir spin densities are defined by $\hat{s}_r^i(\boldsymbol{x}) = \hat{\psi}_{\sigma r}^\dagger(\boldsymbol{x})\tau^i_{\sigma\sigma'}\hat{\psi}_{\sigma' r}(\boldsymbol{x})/2$, where $\hat{\psi}_{\sigma r}(\boldsymbol{x})$ is the annihilation operator for a spin-σ electron in reservoir r at position $\boldsymbol{x}$, τ^i are the Pauli matrices, and $\hat{s}_r^\pm = \hat{s}_r^x \pm i\hat{s}_r^y$. Here, we implicitly assume the dependence of the operators on $\boldsymbol{r}$.

The spin accumulation in the left reservoir leads to an injection of spin current in the form of a superfluid and a thermally activated spin current mediated by magnons. Within the healing length $\ell_h \sim a\sqrt{J/D}$ from the injection site, the latter should transform into supercurrent [19], as the individual magnons cannot carry spin angular momentum along the z axis. The spin current can suffer relaxation in the ferromagnet, which we account for using Gilbert damping phenomenology. For spin waves, the damping rate at $T \ll T_D$ can be estimated as $\tau^{-1} \sim \alpha DS/\hbar$, which defines the magnon ballistic decay length $\ell = v\tau$. We assume $\ell_h \ll \ell$, such that the magnon-mediated current is converted into spin supercurrent without significant decay within the healing length. This imposes a simple condition on Gilbert damping: $\alpha \ll 1$, which is nearly always satisfied in practice.

In order to separate the condensate and thermal contributions to the injected spin current, we parametrize the quantum fields in Eqs. (3) and (4) as a sum of the deterministic classical component (the condensate) and the fluctuating quantum component (magnon cloud): $\hat{\varphi}(\boldsymbol{x}) = \varphi(x,t) + \delta\hat{\varphi}(\boldsymbol{x})$ and $\hat{S}_z(\boldsymbol{x}) = S_z(x,t) + \delta\hat{S}_z(\boldsymbol{x})$ [with a corresponding decomposition for $\hat{n}_z(\boldsymbol{x})$]. The resultant coupling between the two components affects spin transport both within the ferromagnet bulk and at the interfaces. In the bulk, this coupling manifests only at higher orders in the driving field μ_s [20]. At the interfaces, however, the coupling contributes to spin current at linear order in the driving field, as we show below.

To compute the thermal-cloud contribution to spin current through the interface, we insert the above parametrization for $\hat{\varphi}(\boldsymbol{x})$ and $\hat{S}_z(\boldsymbol{x})$ along with the steady-state ansatz $\varphi(x,t) = \varphi(x) + \Omega t$ and $S_z(x,t) = \hbar\Omega/Da^3$ into Eq. (4). The precession frequency Ω now needs to be self-consistently determined in the presence of the thermal cloud. Since the condensate-cloud coupling only leads to nonlinear effects in the bulk (as argued above), linear-response spin transport should be well characterized by the condensate described by the above steady-state solution for φ and S_z together with the decoupled thermal cloud governed by the Hamiltonian $\delta\hat{H}_F = \int d^3\boldsymbol{x}[A(\nabla\delta\hat{\varphi})^2 + K\delta\hat{n}_z^2]/2$.

We first evaluate the condensate contribution to the spin current at each interface. In the absence of the fluctuations, the relevant interaction Hamiltonian is $\hat{V}_0 = \sum_r \hat{V}_{r0}$, with

$$\hat{V}_{r0} = \int \frac{d^2\boldsymbol{k}}{(2\pi)^2}\frac{dk_x}{2\pi}\frac{dk_x'k_x'}{2\pi}\eta_{r0k_xk_x'}e^{i\Omega t}\hat{\psi}^\dagger_{\boldsymbol{k}k_x\uparrow r}\hat{\psi}_{\boldsymbol{k}k_x'\downarrow r} + \text{H.c.}, \tag{5}$$

where $\eta_{r0k_xk_x'} = \eta_r\tilde{S}e^{-if(x_r)}\phi^{r*}_{k_x}(x_r)\phi^r_{k_x'}(x_r)/2$. The reservoir electron operators were expanded as $\hat{\psi}_{\sigma r}(\boldsymbol{x}) = \int\frac{d^2\boldsymbol{k}dk_x}{(2\pi)^3}e^{i\boldsymbol{k}\cdot\boldsymbol{r}}\phi^r_{k_x}(x)\hat{\psi}_{\boldsymbol{k}k_x\sigma r}$, where $\phi^r_{k_x}(x)$ are orthonormal eigenfunctions in the transport direction for the semi-infinite reservoir r. Here, we consider the weak-coupling regime and compute the spin current to lowest nontrivial order in η_r [21]. In Eq. (5), we dropped the z-component exchange, since it does not contribute to the spin current within the weak-coupling treatment. The operator for the spin-current density flowing into each reservoir is

$$\hat{J}^s_{r0} = \frac{i}{2\mathcal{A}}\int\frac{d^2\boldsymbol{k}}{(2\pi)^2}\frac{dk_x}{2\pi}\sum_\sigma[\hat{V}_{r0}, \sigma\hat{\psi}^\dagger_{\boldsymbol{k}k_x\sigma r}\hat{\psi}_{\boldsymbol{k}k_x\sigma r}], \tag{6}$$

where $\mathcal{A}$ is the interface cross-sectional area. From the Kubo formula, we obtain $J^s_{r0} = -(i/\hbar)\int dt'\theta(-t')\times\langle[\hat{J}^s_{r0}(0), \hat{V}_{r0}(t')]\rangle$, where $\theta(t)$ is the Heaviside step function. To linear order in μ_s and $\Omega \propto \mu_s$, we obtain $J^s_{r0} = G^s_r\hbar\Omega_r$, where $\Omega_L = \Omega - \mu_s/\hbar$ and $\Omega_R = \Omega$. (In order to consider spin current into the ferromagnet from

the left reservoir, as in Fig. 1, we must flip the sign of Ω_L.) The conductances read $G_r^s = 2\pi \int_{-\infty}^{\infty} d\varepsilon \nu_r(\varepsilon)[-n'_{\rm FD}(\varepsilon)]$, where $n'_{\rm FD}(\varepsilon) \equiv \partial n_{\rm FD}(\varepsilon)/\partial\varepsilon$ and

$$\nu_r(\varepsilon) = \int \frac{d^2\boldsymbol{k}}{(2\pi)^2}\frac{dk_x}{2\pi}\frac{dk'_x}{2\pi}|\eta_{r0k_xk'_x}|^2\delta(\varepsilon-\epsilon_{\boldsymbol{k}k_xr})\delta(\varepsilon-\epsilon_{\boldsymbol{k}k'_xr}). \tag{7}$$

For the thermal contribution, we expand the interaction to linear order in the fluctuations $\delta\hat{V} = \sum_r \delta\hat{V}_r$ with

$$\delta\hat{V}_r = \int_{\{\boldsymbol{k}\}}{\sum_n}' \eta_{rnk_xk'_x} e^{-i\Omega t}\delta\hat{\varphi}_{\boldsymbol{k}-\boldsymbol{k}'n}\hat{\psi}^\dagger_{\boldsymbol{k}k_x\uparrow r}\hat{\psi}_{\boldsymbol{k}'k'_x\downarrow r} + \text{H.c.}, \tag{8}$$

where $\eta_{rnk_xk'_x} = -i\phi_n^F(x_r)\eta_{r0k_xk'_x}$ and $\int_{\{\boldsymbol{k}\}}$ denotes integral over momenta, $\boldsymbol{k}$, $\boldsymbol{k}'$, k_x, and k'_x, with the appropriate $(2\pi)^{-1}$ factors. Here, we have introduced orthonormal eigenfunctions $\phi_n^F(x) = \sqrt{2/L}\cos(q_n x)$ (with non-negative integers $n \geq 0$ and $q_n = n\pi/L$), which correspond to eigenstates of a free particle in the domain $0 \leq x \leq L$ obeying Neumann boundary conditions, $\partial_x\phi_n^F(0) = 0 = \partial_x\phi_n^F(L)$. The spin-wave operators are expanded as $\delta\hat{\varphi}(\boldsymbol{x}) = \int(d^2\boldsymbol{q}/(2\pi)^2)\sum_n' e^{i\boldsymbol{q}\cdot\boldsymbol{r}}\phi_n^F(x)\delta\hat{\varphi}_{\boldsymbol{q}n}$, with an analogous expansion for $\delta\hat{S}_z(\boldsymbol{x})$. We use prime on the summation sign to indicate that it excludes uniform (i.e., condensate) mode with $\boldsymbol{q} = 0$ and $n = 0$. The magnon current-density operator $\delta\hat{\boldsymbol{J}}_r^s$ is then given by the right-hand side of Eq. (6) but with $\hat{V}_{r0}$ replaced by $\delta\hat{V}_r$. The steady-state magnon spin current across the interface is then similarly obtained through $\delta J_r^s = -(i/\hbar)\int dt'\theta(-t')\langle[\delta\hat{J}_r^s(0), \delta\hat{V}_r(t')]\rangle$.

The Hamiltonian for the fluctuations $\delta\hat{H}_F$ can be diagonalized using the ladder operators $\hat{a}_{\boldsymbol{q}n}$ and $\hat{a}^\dagger_{\boldsymbol{q}n}$ obeying $[\hat{a}_{\boldsymbol{q}n}, \hat{a}^\dagger_{\boldsymbol{q}'n'}] = (2\pi)^2\delta(\boldsymbol{q}-\boldsymbol{q}')\delta_{nn'}$. We obtain $\delta\hat{H}_F = \int(d^2\boldsymbol{q}/(2\pi)^2)\sum_n' E_{\boldsymbol{q}n}(\hat{a}^\dagger_{\boldsymbol{q}n}\hat{a}_{\boldsymbol{q}n} + 1/2)$, where the magnon spectrum is $E_{\boldsymbol{q}n} = \hbar v\sqrt{|\boldsymbol{q}|^2 + q_n^2}$. In this basis, the phase field reads $\delta\hat{\varphi}_{\boldsymbol{q}n} = \sqrt{Da^3/2E_{\boldsymbol{q}n}}(\hat{a}^\dagger_{-\boldsymbol{q}n} + \hat{a}_{\boldsymbol{q}n})$. The linearized thermal contribution to the injected spin-current density reads $\delta J_r^s = \delta G_r^s\hbar\Omega_r$, where the magnon conductances are given by $\delta G_r^s = 4\pi\int_0^\infty d\varepsilon\varepsilon\delta\nu_r(\varepsilon)[-n'_{\rm BE}(\varepsilon)]$, in terms of

$$\delta\nu_r(\varepsilon) = \int_{\{\boldsymbol{k}\}}{\sum_n}' |\eta_{rnk_xk'_x}|^2 B_{\boldsymbol{k}-\boldsymbol{k}'n}(\varepsilon)\delta(\mu-\varepsilon_{\boldsymbol{k}k_xr})\delta(\mu-\varepsilon_{\boldsymbol{k}'k'_xr}), \tag{9}$$

and the magnon spectral function $B_{\boldsymbol{q}n}(\varepsilon) = (Da^3/2E_{\boldsymbol{q}n})\delta(\varepsilon - E_{\boldsymbol{q}n})$. Here, $n'_{\rm BE}(\varepsilon) \equiv \partial n_{\rm BE}(\varepsilon)/\partial\varepsilon$, $n_{\rm BE}(\varepsilon) = (e^{\beta\varepsilon}-1)^{-1}$, and we assumed that $\mu \gg k_BT$. The total injected spin-current density is then given by $J_r^s = \mathcal{G}_r^s\hbar\Omega_r$, where $\mathcal{G}_r^s = G_r^s + \delta G_r^s$. This is a main result of our microscopic calculation. Because of Gilbert damping in the ferromagnetic bulk, the injected spin current J_L^s and the collected spin current J_R^s are related via $J_L^s - J_R^s = \Delta J^s$, where $\Delta J^s = \alpha s\Omega L$ is the condensate spin relaxation in the bulk. Since the total injected spin current is fully transformed into supercurrent in the bulk, we, thus, reproduce Eqs. (2) with the substitution $g_r^{\uparrow\downarrow} \to 4\pi\mathcal{G}_r^s$.

In order to quantify the thermal contribution to the spin transfer with respect to the coherent contribution, we evaluate the ratio $\mathcal{R} \equiv \delta G_r^s/G_r^s$. In the low-temperature regime considered thus far (i.e., $T \ll T_D, T_c$), we obtain $\mathcal{R} = (\sqrt{S}/6)\sqrt{T/T_D}(T/T_c)^{3/2}$, where $T_c = JS^2/k_B$ and $T_D = DS/k_B$ (see the Supplemental Material [18] for details). Here, we see that the thermal contribution to the spin transfer is very small. In the high-temperature regime, $T_D \ll T \ll T_c$, thermal magnons are no longer strongly affected by the planar anisotropy and, thus, acquire a circular character. In this case, the ratio of the thermal to condensate spin currents becomes $\mathcal{R}^c = (\sqrt{S}/2\pi^2)\Gamma(5/2)\zeta(3/2)(T/T_c)^{3/2}$, where Γ is the gamma function, and ζ is the Riemann zeta function (see the Supplemental Material [18] for details). We see that the thermal contribution remains small as long as $T \ll T_c$.

Discussion.—The superfluid spin transport can be detected using the setup shown in Fig. 1. Here, the ferromagnet is sandwiched by identical metals with strong spin-orbit coupling characterized by an effective spin Hall angle $\theta_{\rm SH}$ at the ferromagnet|metal interfaces. Let J_R^c denote the charge-current density produced via the inverse spin Hall effect in the right metal given the applied charge-current density J_L^c in the left metal, which define the (negative) drag coefficient $\mathcal{D} \equiv -J_R^c/J_L^c$. The spin current impinging on the static ferromagnet at the left interface is given by $J_{\rm SH}^s = (\hbar/2e)\theta_{\rm SH}J_L^c$. Using Onsager reciprocity, the induced charge-current density reads $J_R^c = -(\theta_{\rm SH}\sigma/d)\hbar\Omega/2e$, where σ (d) are the conductivity (thickness) of the right metal; here, we assume $d \gtrsim \lambda_{\rm sf}$, where $\lambda_{\rm sf}$ is the spin-flip length of the metal. In the absence of magnetic losses and assuming $\theta_{\rm SH} \ll 1$, $J_R^s = J_L^s = J_{\rm SH}^s/2$, which gives $\hbar\Omega = (2\pi/g^{\uparrow\downarrow})J_{\rm SH}^s$ resulting in $\mathcal{D}_0 = \theta_{\rm SH}^2\sigma/2g_Qg^{\uparrow\downarrow}d$, where $g_Q \equiv 2e^2/h$. In the presence of losses, the precession frequency is suppressed according to Eq. (2) as $\hbar\Omega = [4\pi/(2g^{\uparrow\downarrow} + g_\alpha)]J_{\rm SH}^s$, which results in $\mathcal{D} = \mathcal{D}_0/(1 + L/L_\alpha)$, where $L_\alpha \equiv \hbar g^{\uparrow\downarrow}/2\pi\alpha s$. At finite temperatures, the mixing conductance acquires a thermal contribution, $g^{\uparrow\downarrow}|_{T\neq 0} = (1+\mathcal{R})g^{\uparrow\downarrow}|_{T=0}$, which we parametrize by $\mathcal{R}(T)$. We summarize these results in Fig. 2.

For a quantitative estimate, we consider a Pt|YIG|Pt hybrid structure (which appears to be a promising combination because of strong spin-orbit coupling in Pt and low Gilbert damping and weak magnetic anisotropy in YIG). Using $\theta_{\rm SH} \sim 0.1$ (measured for a platinum|permalloy interface [22]), $\sigma \sim 0.1(\mu\Omega\times{\rm cm})^{-1}$ for Pt, $d \approx \lambda_{\rm sf} \sim 1$ nm (spin-flip length in Pt [22]), and $g^{\uparrow\downarrow} \sim 5\times 10^{18}$ m^{-2} for the YIG|Pt interfaces [23], we get $\mathcal{D}_0 \sim 0.1$ [24]. Taking $\alpha \sim 10^{-4}$ and using YIG spin density $s/\hbar \sim 10^{22}$ cm^{-3} [25], we get for the crossover length $L_\alpha \sim 1$ μm. The large and long-ranged negative drag constitute our key predictions.

Finally, we remark that breaking of the U(1) symmetry within the easy plane of the ferromagnet is detrimental to

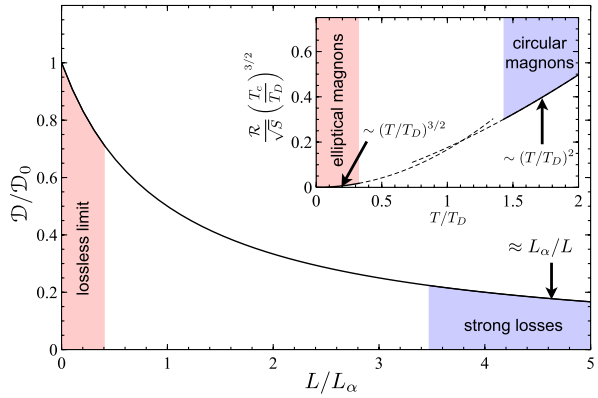

FIG. 2 (color online). Negative drag coefficient normalized by its lossless value $\mathcal{D}_0 = \theta_{\rm SH}^2\sigma/2g_Q g^{\uparrow\downarrow}d$ as a function of the length of the ferromagnet L. (Inset) Normalized thermal correction $\mathcal{R} = \delta g^{\uparrow\downarrow}(T)/g^{\uparrow\downarrow}|_{T=0}$ to the spin-mixing conductance as a function of the ambient temperature T.

the dc spin-carrying superfluid state studied here. Relevant macroscopic manifestations of this symmetry breaking are Gilbert damping, which has already been accounted for, and magnetic anisotropy. In the presence of the latter, the applied current must overcome a threshold in order to establish the spin superfluid-carrying state over the length of the ferromagnet. However, the applied current cannot exceed an upper critical current, beyond which the induced planar magnetic spiral state becomes unstable [12,19].

The authors would like to thank Bertrand I. Halperin and Mircea Trif for illuminating discussions. This work was supported in part by FAME (a SRC STARnet center sponsored by MARCO and DARPA), the NSF under Grants No. DMR-0840965 and No. 228481 from the Simons Foundation. This research was supported in part by the Kavli Institute for Theoretical Physics through Grant No. NSF PHY11-25915.

[1] I. Žutić, J. Fabian, and S. Das Sarma, Rev. Mod. Phys. **76**, 323 (2004).
[2] A. Khitun, M. Bao, and K. L. Wang, IEEE Trans. Magn. **44**, 2141 (2008).
[3] Y. Kajiwara, K. Harii, S. Takahashi, J. Ohe, K. Uchida, M. Mizuguchi, H. Umezawa, H. Kawai, K. Ando, K. Takanashi, S. Maekawa, and E. Saitoh, Nature (London) **464**, 262 (2010); K. Uchida, J. Xiao, H. Adachi, J. Ohe, S. Takahashi, J. Ieda, T. Ota, Y. Kajiwara, H. Umezawa, H. Kawai, G. E. W. Bauer, S. Maekawa, and E. Saitoh, Nat. Mater. **9**, 894 (2010).
[4] T. Nikuni, M. Oshikawa, A. Oosawa, and H. Tanaka, Phys. Rev. Lett. **84**, 5868 (2000); A. Oosawa, M. Ishii, and H. Tanaka, J. Phys. Condens. Matter **11**, 265 (1999).
[5] T. Radu, H. Wilhelm, V. Yushankhai, D. Kovrizhin, R. Coldea, Z. Tylczynski, T. Lühmann, and F. Steglich, Phys. Rev. Lett. **95**, 127202 (2005).
[6] S. O. Demokritov, V. E. Demidov, O. Dzyapko, G. A. Melkov, A. A. Serga, B. Hillebrands, and A. N. Slavin, Nature (London) **443**, 430 (2006).
[7] B. I. Halperin and P. C. Hohenberg, Phys. Rev. **188**, 898 (1969).
[8] L. R. Corruccini and D. D. Osheroff, Phys. Rev. Lett. **34**, 564 (1975); M. Vuorio, J. Phys. C **7**, L5 (1974); **9**L267 (1976); E. B. Sonin, JETP Lett. **30**, 662 (1979).
[9] A. S. Borovik-Romanov, Y. M. Bunkov, V. V. Dmitriev, and Y. M. Mukharskii, JETP Lett. **40**, 1033 (1984); I. A. Fomin, JETP Lett. **40**, 1037 (1984).
[10] E. B. Sonin, Solid State Commun. **25**, 253 (1978).
[11] R. R. Guseinov and L. V. Keldysh, JETP Lett. **36**, 1193 (1973).
[12] J. König, M. C. Bønsager, and A. H. MacDonald, Phys. Rev. Lett. **87**, 187202 (2001).
[13] S. Murakami, N. Nagaosa, and S.-C. Zhang, Science **301**, 1348 (2003).
[14] J. Sinova, D. Culcer, Q. Niu, N. A. Sinitsyn, T. Jungwirth, and A. H. MacDonald, Phys. Rev. Lett. **92**, 126603 (2004).
[15] Y. Tserkovnyak, A. Brataas, and G. E. W. Bauer, Phys. Rev. Lett. **88**, 117601 (2002); Y. Tserkovnyak, A. Brataas, G. E. W. Bauer, and B. I. Halperin, Rev. Mod. Phys. **77**, 1375 (2005).
[16] J. C. Slonczewski, J. Magn. Magn. Mater. **159**, L1 (1996).
[17] S. S.-L. Zhang and S. Zhang, Phys. Rev. Lett. **109**, 096603 (2012).
[18] See Supplemental Material at http://link.aps.org/supplemental/10.1103/PhysRevLett.112.227201 for how the ratios $\mathcal{R}$ and $\mathcal{R}^c$ are obtained, it then briefly studies spin transport when the spin accumulation is oriented parallel to the ferromagnet's easy-plane.
[19] E. B. Sonin, Sov. Phys. JETP **47**, 1091 (1978); Adv. Phys. **59**, 181 (2010).
[20] In the high-temperature (circular-magnon) regime, $T_D \ll T$, the bulk coupling between a long-wavelength condensate dynamics and thermal cloud acquires a particularly simple form. In this case, magnons experience reactive and dissipative spin-motive forces, whose Cartesian components are proportional to $\boldsymbol{n}\cdot(\partial_t\boldsymbol{n}\times\nabla_i\boldsymbol{n})$ [26] and $\partial_t\boldsymbol{n}\cdot\nabla_i\boldsymbol{n}$ [27], respectively. Since both $\partial_t\boldsymbol{n}$ and $\nabla_i\boldsymbol{n}$ are linear in the nonequilibrium drive, the effects of these forces would appear only at quadratic order.
[21] The weak-coupling regime can be justified here if the energy scale associated with the interface exchange coupling, i.e., η_r/a^4 is much smaller than the typical magnon energy scale $\varepsilon_m \sim \max\{k_BT, DS\}$ or the typical energy scale of the conduction electrons in the reservoir, which is the Fermi energy ε_F. Since we expect $\varepsilon_m \ll \varepsilon_F$, the weak-coupling treatment should be valid for $\eta_r/a^4 \ll \epsilon_m$.
[22] L. Liu, T. Moriyama, D. C. Ralph, and R. A. Buhrman, Phys. Rev. Lett. **106**, 036601 (2011).
[23] C. Burrowes, B. Heinrich, B. Kardasz, E. A. Montoya, E. Girt, Y. Sun, Y.-Y. Song, and M. Wu, Appl. Phys. Lett. **100**, 092403 (2012).
[24] For purely magnon-mediated drag in a Pt|YIG|Pt hybrid structure, the drag coefficient has been theoretically proposed and estimated to be $\sim 10^{-4}$ [17]. Reference [3] reported a drag $\sim 10^{-9}$ in a Pt|YIG|Pt system (which was interpreted to develop as a result of a nonlinear magnon generation).
[25] S. Bhagat, H. Lessoff, C. Vittoria, and C. Guenzer, Phys. Status Solidi **20**, 731 (1973).
[26] G. E. Volovik, J. Phys. C **20**, L83 (1987).
[27] R. A. Duine, Phys. Rev. B **77**, 014409 (2008); Y. Tserkovnyak and M. Mecklenburg, Phys. Rev. B **77**, 134407 (2008).